Available online at www.sciencedirect.com
ScienceDirect
International Journal of Multiphase Flow 34 (2008) 547–558
International Journal of Multiphase Flow
www.elsevier.com/locate/ijmulflow

On the use of Csanady's formulae in a turbulent gas–solid channel flow

B. Arcen, A. Tanière *

LEMTA, Nancy-University, CNRS, ESSTIN, 2 rue Jean Lamour, F-54529 Vandoeuvre-lès-Nancy, France

Received 15 May 2007; received in revised form 4 October 2007

Abstract

The paper examines the use of expressions proposed by Csanady to predict the influence of the crossing trajectory and continuity effects on the decorrelation time scales of the fluid along solid particle trajectories in horizontal and downward vertical channel flows. The model is evaluated using data provided by a direct numerical simulation (DNS) of the carrier phase combined with a Lagrangian simulation of discrete particle (LS). Two particle relaxation times and two values of the gravity acceleration are considered. The results show the possibility of using Csanady's expressions in a turbulent channel flow provided that the spatial and temporal correlations anisotropy is included in the model. As in isotropic homogeneous turbulence, a decrease of the decorrelation time scales is found to be more important in the directions perpendicular to the mean relative velocity.

Keywords: Gas–solid flow; Crossing trajectory and continuity effects; Non-homogeneous turbulence; Dispersion

1. Introduction

The numerical simulation of particle-laden flows necessitates the use of a dispersion model when only the averaged velocity of the carrier phase is known (Simonin, 2000; Oesterlé and Zaichik, 2004). The key issue of dispersion models lies in building a proper stochastic process for the prediction of the velocity of the fluid seen by a discrete particle. In the frame of three-dimensional dispersion model, the fluctuating velocity time increment of the fluid seen can be expressed by means of a Langevin-type equation (Simonin, 2000; Minier and Peirano, 2001; Reeks, 2005). It is then necessary to specify its coefficients, i.e. the drift and diffusion terms. In homogeneous isotropic turbulence, the drift term is the inverse of a time scale which can be shown to represent exactly the integral time of the fluid seen (Minier and Peirano, 2001). In non-homogeneous turbulence as in a channel flow, such a modelling idea in the stochastic model can be retained, but locally in space. In this case, the time scale, T^*_{ij} can be regarded as a local decorrelation of the fluid velocity fluctuation along the discrete particle path provided that the calculation of the velocity correlation is conditioned by the initial particle location. Whatever the properties of the turbulence, this fluid velocity temporal decorrelation along discrete particle path is all the more important as the fluid and particle mean velocity differ due to an external force field (the so-called crossing trajectory effect). In isotropic homogeneous turbulence, various methods have been suggested to estimate the diagonal time scales T^*_{ii} in terms of the particle inertia and of the mean relative velocity between the particles and the fluid (Wang and Stock, 1993; Derevich, 2000, 2001). Nevertheless, the formulae of Csanady (1963) remains the reference model at the moment in two-phase

* Corresponding author. Tel.: +33 383 685 083.
E-mail address: anne.taniere@esstin.uhp-nancy.fr (A. Tanière).

0301-9322/$ - see front matter © 2008 Elsevier Ltd. All rights reserved.
doi:10.1016/j.ijmultiphaseflow.2008.01.001

flow modelling (Sawford and Guest, 1991; Wilson, 2000; Minier et al., 2004; Reynolds, 2004).

Csanady worked essentially on asymptotic particle dispersion rates in the atmosphere where the temporal and length scales are very large. He focused on the behavior of the space–time velocity correlation of falling particles in the direction parallel to the mean relative velocity, noted $\mathbf{V}_r$. Neglecting the inertia effect, assuming isotropic and stationary turbulence, and using a coordinate system moving with the mean flow, Csanady (1963) reduced this velocity space–time correlation in a non-dimensional form which depends on three parameters: the magnitude of the mean relative velocity $\|\mathbf{V}_r\|$, the fluid turbulent agitation $\langle u'^2\rangle^{1/2}$ and an Eulerian length scale. All of them are associated with the parallel direction of the mean relative velocity, which is necessarily aligned with the gravity vector in Csanady's study. Then, he assumed that the velocity correlation of the fluid along a heavy particle trajectory is an interpolation between two limit cases. The first one is related to the correlation of the fluid seen which tends to the fluid Lagrangian one when the relative motion is negligible, i.e. when $\|\mathbf{V}_r\|/\langle u'^2\rangle^{1/2} \ll 1$. In the second case, the correlation of the fluid seen tends to an Eulerian velocity correlation when the relative motion is dominant, i.e. $\|\mathbf{V}_r\|/\langle u'^2\rangle^{1/2} \gg 1$. This result is derived under a frozen turbulence hypothesis. These two asymptotic cases allow him to suggest that in the direction parallel to the mean relative velocity, called longitudinal direction, the lines of constant space–time correlation for longitudinal separation and time lag are ellipses. An exponential-decay function is then used to describe the correlation coefficient.

For the particle dispersion in the directions perpendicular to the mean relative velocity, attention has been paid by Csanady to reflect the continuity effect. As mentioned by Csanady, a particularly serious consequence of the crossing trajectory effect occurs in connection with the perpendicular directions to the mean relative velocity (called lateral directions in its paper), i.e. the continuity effect. According to the fluid mass balance equation, the presence of negative loops in the shape of the lateral velocity correlation curves of the fluid seen is necessary. In physical terms, the continuity effect causes a decrease of the decorrelation time scales for lateral dispersion which is more important than in the longitudinal one. In order to reproduce the negative loop in the velocity correlation function, Csanady used a temporal analogy with the famous isotropic relationships between the longitudinal and lateral two-points space correlation, namely $f(r)$ and $g(r)$. However, using such a type of correlation implies the existence of only two turbulence length scales, one longitudinal and one lateral, noted, respectively L_f and L_g, where L_f is twice larger than L_g. These length scales were included in Csanady's analysis in order to take the continuity effect into consideration. Finally, Csanady (1963) proposed the following couple of expressions for modelling the time scales of the fluctuating fluid velocity seen components parallel and perpendicular to the mean relative velocity, noted $T_{\parallel}^{*g}$ and $T_{\perp}^{*g}$

$$T_{\parallel}^{*g} = T^{\mathrm{L}}\left[1+\left(\frac{\|\mathbf{V}_r\|T^{\mathrm{L}}}{L_f}\right)^2\right]^{-1/2},$$
$$T_{\perp}^{*g} = T^{\mathrm{L}}\left[1+\left(\frac{\|\mathbf{V}_r\|T^{\mathrm{L}}}{L_g}\right)^2\right]^{-1/2}, \quad (1)$$

where T^{L} is the fluid Lagrangian integral time scale (which is assumed to be equal to the moving Eulerian time scale according to Csanady's analysis in the atmosphere). The presence of a factor 4 appears in the above expression of $T_{\perp}^{*g}$ if it is written in terms of L_f instead of L_g, due to the isotropic relationship $L_f = 2L_g$.

In the atmosphere, the use of this isotropic relation is questionable according to Csanady. However, if we refer, as him, to the results of the spatial correlations of Grant (1958) in a turbulent boundary layer, or to the results of Comte-Bellot (1965) and Kim et al. (1987), in a channel flow, two functional forms of the correlation are predominant: an exponential-decay for the longitudinal correlations and an exponential curve with negative loops for the lateral correlations. This has lead us to consider the heuristic approach developed by Csanady in a channel flow, where there are fifteen different non-zero two-points space correlations which are qualitatively similar to those encountered in isotropic turbulence. That is why, we think that in a non-homogeneous turbulence, it is easier to use Csanady's work in order to extend the prediction of the influence of the crossing trajectory and continuity effects on the decorrelation time scale of the fluid seen to more complex turbulent flows than the other modelling attempts. For example, recently, Thomas and Oesterlé (2005) in a turbulent linear shear flow, attempted to describe precisely the crossing trajectory effect on the decorrelation time scales of the fluid seen. This study shows the difficulty to theoretically obtain analytic expressions to model the crossing trajectory effect in anisotropic turbulence.

Although the flow studied here is a non-homogeneous turbulent channel flow, we propose in the present paper to retain the basic lines of Csanady's analysis, and to model the diagonal time scales of the fluid seen using an analogous functional form as in Eq. (1). It should be noted that the decorrelation time scales considered here are not tensors. The questions which are addressed in this paper are:"Is it possible to correctly model the crossing trajectory and continuity effects using expressions based on those proposed by Csanady in a turbulent complex flow ?" and if the results are not satisfactory in non-homogeneous flows, is it due to the functional form or is it due to a crude estimate of the parameters appearing in these expressions ?

2. Crossing trajectory effect: extension of Csanady's formulae

The expressions predicting the decorrelation time scales of the fluid seen examined here are derived from those proposed by Deutsch (1992) who introduced the inertia effect

into Csanady's theory. He assumed that, when $\|\mathbf{V}_r\|/\langle u'^2\rangle^{1/2} \ll 1$, the velocity correlation of the fluid seen tends to the correlation of the fluid seen obtained in the absence of the gravity, noted $T^{*g}(g=0)=T^*$, and not to the Lagrangian one. Hence, Deutsch (1992) proposed to link the two limit cases by substituting T^L by T^* in Eq. (1).

Knowing that these expressions have been developed for isotropic turbulence whereas the flow studied here is strongly anisotropic, some modifications and assumptions have to be made. The first modification is to consider the anisotropic character of the time scales of the fluid seen when no external force is acting on particles, T^* is then replaced by T^*_{ij} and T^{*g} by T^{*g}_{ij} in Eq. (1). The length scales $L^{(k)}_{ij}$, where k denotes the direction of the separation between the two points, are introduced instead of L_f or L_g in order to take the anisotropy of the turbulence into account. Moreover, the reference system in Csanady or Deutsch analysis has been chosen so that one of its axes is parallel to the external force (i.e. gravity force) and thus aligned with the mean relative velocity direction. In the present non-homogeneous flow, the mean relative velocity vector is inclined with respect to the gravity direction which is aligned with one of the axes of the coordinate system. Consequently, in order to apply Csanady's analysis whatever the configuration of the flow (horizontal and vertical), only the component of the mean relative velocity which is parallel to the gravity direction will be considered.

Under these considerations, the modified expressions are

$$\begin{aligned} T^{*g}_{ii} &= T^*_{ii}\left[1+\left(\frac{V_{r,i}T^*_{ii}}{L^{(i)}_{ii}}\right)^2\right]^{-1/2}, \\ T^{*g}_{jj} &= T^*_{jj}\left[1+\left(\frac{V_{r,i}T^*_{jj}}{L^{(i)}_{jj}}\right)^2\right]^{-1/2}, \end{aligned} \tag{2}$$

where the index i indicates the gravity direction whereas j ($\neq i$) represents the directions perpendicular to the gravity. Note that if we consider $L^{(i)}_{ii}/L^{(i)}_{jj}=2$, the expressions of Csanady are recovered, namely

$$\begin{aligned} T^{*g}_{ii} &= T^*_{ii}\left[1+\left(\frac{V_{r,i}T^*_{ii}}{L^{(i)}_{ii}}\right)^2\right]^{-1/2}, \\ T^{*g}_{jj} &= T^*_{jj}\left[1+4\left(\frac{V_{r,i}T^*_{jj}}{L^{(i)}_{ii}}\right)^2\right]^{-1/2}. \end{aligned} \tag{3}$$

We propose to study these two couples of expressions, Eqs. (2) and (3), in which the continuity effect is treated differently. The spatial and temporal correlations are computed following the conventional definitions, respectively:

$$L^{(k)}_{ij} = \int_0^\infty R^{(k)}_{ij}\,\mathrm{d}r \quad \text{and} \quad T^*_{ij} = \int_0^\infty R^*_{ij}\,\mathrm{d}\tau \tag{4}$$

with

$$\begin{aligned} R^{(k)}_{ij}(\mathbf{x},r,t) &= \frac{\left\langle u'_i(\mathbf{x},t)u'_j(\mathbf{x}+r\mathbf{e}_\mathbf{k},t)\right\rangle}{\sqrt{\langle u'^2_i(\mathbf{x},t)\rangle}\sqrt{\langle u'^2_j(\mathbf{x}+r\mathbf{e}_\mathbf{k},t)\rangle}}, \\ R^*_{ij}(\mathbf{x}_\mathrm{p}(t),\tau) &= \frac{\left\langle u'_i(\mathbf{x}_\mathrm{p}(t),t)u'_j(\mathbf{x}_\mathrm{p}(t+\tau),t+\tau)\right\rangle}{\sqrt{\langle u'^2_i(\mathbf{x}_\mathrm{p}(t),t)\rangle}\sqrt{\langle u'^2_j(\mathbf{x}_\mathrm{p}(t+\tau),t+\tau)\rangle}}, \end{aligned} \tag{5}$$

where $\mathbf{x}_\mathrm{p}$ is the solid particle position and r is the separation between two points.

3. Channel flow DNS and solid particle tracking

3.1. Numerical parameters of the DNS computations

The DNS solver, second-order accurate in space and in time (Orlandi, 2000), performs the simulation of a turbulent channel flow at $Re_b = 2800$ (based on channel half-width δ and bulk velocity U_b) corresponding to a Reynolds number based on the wall-shear velocity, Re_τ, equals to approximately 185. The subscripts 1, 2 and 3 refer to the streamwise (x), wall-normal (y) and spanwise (z) directions, respectively. Two different domain sizes are used for the horizontal and downward vertical channel flows. Numerical parameters are summed up in Table 1. The superscript $(\cdot)^+$ will denote hereafter quantities normalized with the wall shear-velocity $u_\tau = 0.027$ m s^{-1} and the kinematic viscosity $\nu = 1.5\times10^{-5}$ m^2 s^{-1}. The channel flow being statistically homogeneous in the streamwise and spanwise directions, periodic boundary conditions are applied in these directions. The time discretisation is semi-implicit, i.e. the non-linear terms are written explicitly with the third-order Runge–Kutta scheme and the viscous terms are written implicitly using a Crank–Nicolson scheme. In the wall-normal direction, the mesh is stretched according to a hyperbolic tangent whereas a uniform mesh is applied in the streamwise and spanwise directions.

3.2. Dispersed phase

The numerical simulation of solid particle trajectories is restricted to spherical particles smaller than the dimension of the smallest cell $\Delta y^+ = 1$ and consequently smaller than

Table 1
Numerical simulation parameters. L_x, L_y and L_z are the domain dimensions; N_x, N_y and N_z are the number of grid points; Δx^+, Δy^+ and Δz^+ are the grid spacings in wall units. Δt^+ is the time step in wall units

	Horizontal flow	Downward vertical flow
Re_τ	≈185	≈185
L_x, L_y, L_z	$2.5\pi\delta$, 2δ, $1.5\pi\delta$	$2\pi\delta$, 2δ, $1.5\pi\delta$
N_x, N_y, N_z	192, 129, 160	192, 151, 160
Δx^+, Δy^+, Δz^+	7.6, [1,4.6], 5.4	6, [0.35,5.2], 5.4
Δt^+	≈0.1	≈0.03

the smallest Kolmogorov length scale. The solid particle volume fraction is assumed to be relatively small and particle–particle interactions are neglected. In addition, considering that the ratio between the particle and fluid density obeys $\rho_p/\rho \gg 1$, the particle equation of motion can be written without taking the added mass, history and spin induced lift forces into account. Consequently, under these considerations and taking the gravitational acceleration $\mathbf{g}$ into account, the equation governing the motion of a solid particle is

$$\frac{dv_i}{dt} = \frac{\tilde{u}_i - v_i}{\tau_p} + \frac{F_i^L}{m_p} + g_i, \tag{6}$$

where F_i^L represents the shear-induced lift force, m_p is the mass of a single particle, v_i are the particle's velocity components, and $\tilde{u}_i(t) = u_i(\mathbf{x_p}(t), t)$ are the fluid velocity components interpolated at the solid particle's location using a 3D Hermite interpolation. The aerodynamic forces considered here are the non-linear drag and the shear-induced lift force, both of them are corrected for near-wall effects (Arcen et al., 2006). The particle relaxation time τ_p is expressed in terms of the drag coefficient C_D and of the magnitude of the relative velocity. The particle equation of motion is time integrated using the third-order Runge–Kutta scheme. The total number of particles is 640,000 in the horizontal configuration whereas 300,000 are used in the vertical one. Initially, particles are introduced with the same velocity as the surrounding fluid. Statistics on the dispersed phase were started after a time lag of approximately $t^+ = 600$ in the horizontal case and of $t^+ = 6000$ in the downward flow in order to get results independent of the imposed initial conditions; these time lags being the necessary time for particle statistics (with the exception of the mean concentration) to reach a stationary state. Concerning the smooth wall boundary conditions of the dispersed phase, perfectly elastic collisions are assumed. Furthermore, as soon as particles moved out of the computational domain, they are re-introduced via periodic boundary conditions. The numerical predictions of the present code has been evaluated, in the frame of an international test case, against the DNS-LS data issuing from the computational codes of Marchioli et al. (2007). The comparison of the results issuing from these DNS-LS codes, which are based on different numerical methods, has shown the accuracy of the present code.

In order to distinguish the crossing trajectory and inertia effects, the following dimensionless quantities have been chosen to characterize the motion of the dispersed phase: d_p^+ (particle diameter), τ_p^+ [with τ_p defined in the Stokes regime as $\tau_p = (\rho_p d_p^2)/(18\mu)$], and $\tau_p^+ g^+$. In a quiescent gas flow, $\tau_p g$ is the terminal velocity of a solid particle. The inertia effect is studied using two values of the particle inertia, $\tau_p^+ = 1.2$ and 15.4. The effect of the gravity acceleration is investigated by conducting simulations for two values of the gravity parameter, $\tau_p^+ g^+ = 1$ or 2. The dispersed characteristics are summed up in Table 2.

Table 2
Dispersed phase characteristics

Case	d_p (μm)	d_p/δ	ρ_p/ρ	τ_p^+	$\tau_p^+ g^+$
1	50	0.0005	2500	1.2	1
2	140	0.0014	4166	15.4	1
3	50	0.0005	2500	1.2	2
4	140	0.0014	4166	15.4	2

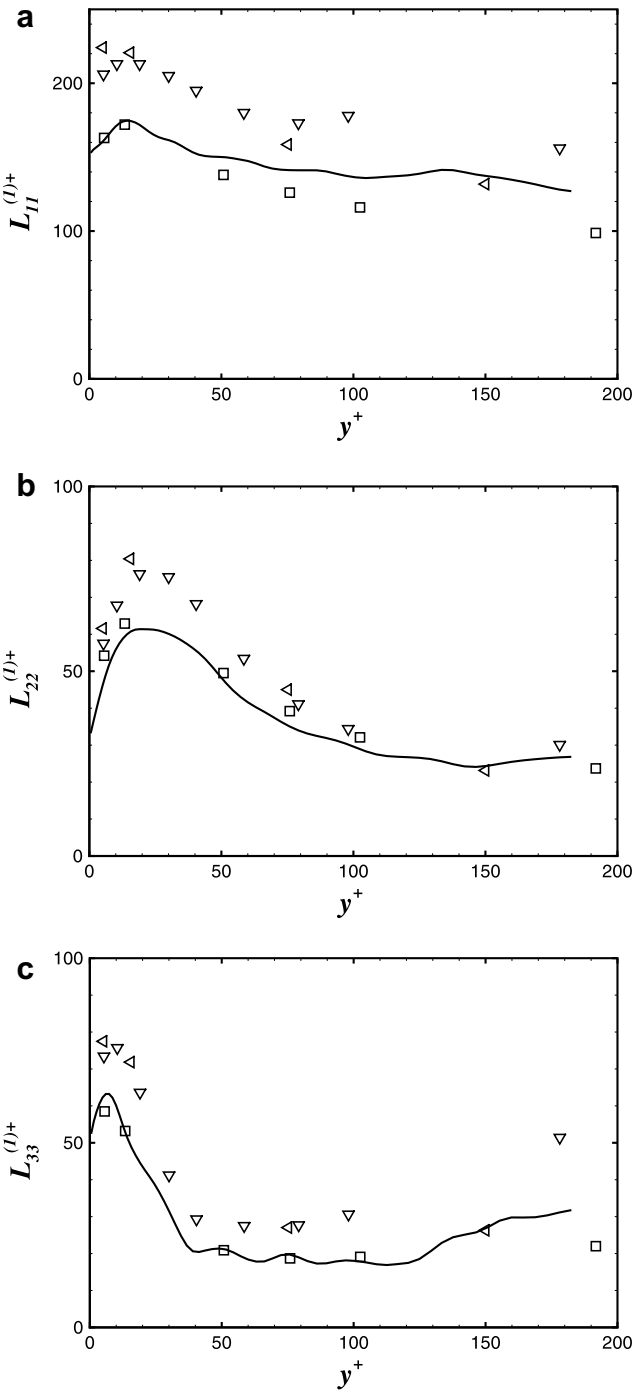

Fig. 1. Streamwise integral length scales $L_{ij}^{(1)}$. (a) $L_{11}^{(1)}$. (b) $L_{22}^{(1)}$. (c) $L_{33}^{(1)}$. (—) presents results; (▽) Moser et al. (1999); (◁) Iwamoto (2002); (□) Kristoffersen and Andersson (1993).

4. Assessment of spatial correlations

In order to apply Eqs. (2) and (3) in the horizontal and downward vertical channel flows, the integral length scales associated with a streamwise and wall-normal displacement are necessary. We propose here to compare the results obtained for these length scales issuing from our DNS computation with the data given by Kristoffersen and Andersson (1993); Moser et al. (1999) and Iwamoto (2002). The length scales obtained from the streamwise and wall-normal two-points velocity correlation functions are noted $L_{ij}^{(1)}$ and $L_{ij}^{(2)}$, respectively. Since the spatial correlations in the streamwise direction are symmetric, the corresponding integral length scales are numerically estimated by

$$L_{ij}^{(1)} = \int_0^{L_1/2} R_{ij}^{(1)}\,\mathrm{d}r. \tag{7}$$

This is not the case in the wall-normal direction. Therefore, we propose to distinguish two different integral length scales by integrating $R_{ij}^{(2)}$ from a point located at y (at which the spatial correlation has been calculated) to the upper or lower wall, as

$$L_{ij}^{(2-)} = \int_{-\delta}^{y} R_{ij}^{(2)}\,\mathrm{d}r \quad \text{and} \quad L_{ij}^{(2+)} = \int_{y}^{\delta} R_{ij}^{(2)}\,\mathrm{d}r. \tag{8}$$

Results related to $L_{ij}^{(1)}$ and $L_{ij}^{(2)}$ are presented in Figs. 1 and 2 as a function of y^+ (the bottom wall is located at $y^+ = 0$). We observed that the streamwise length scales, $L_{11}^{(1)}$, $L_{22}^{(1)}$ and $L_{33}^{(1)}$, issuing from our DNS as well as those deduced from the spatial correlation data of Kristoffersen and Andersson (1993) are slightly smaller than the length scales obtained by Moser et al. (1999) and Iwamoto (2002), which are in good accordance for $y^+ < 100$. The wall-normal length scales $L_{ij}^{(2-)}$ and $L_{ij}^{(2+)}$ are reported in Fig. 2(a) and (b). We note the dissymmetric character of these length scales since $L_{ij}^{(2+)}$ differs clearly from $L_{ij}^{(2-)}$. In the near-wall region, the values of $L_{ij}^{(2+)}$ are found to be higher than the values of $L_{ij}^{(2-)}$, whereas near the channel center, logically, $L_{ij}^{(2-)}$ tend to $L_{ij}^{(2+)}$. Moreover, as it can be seen from Figs. 1 and 2, the streamwise length scales are slightly higher than those obtained in the wall-normal direction. The

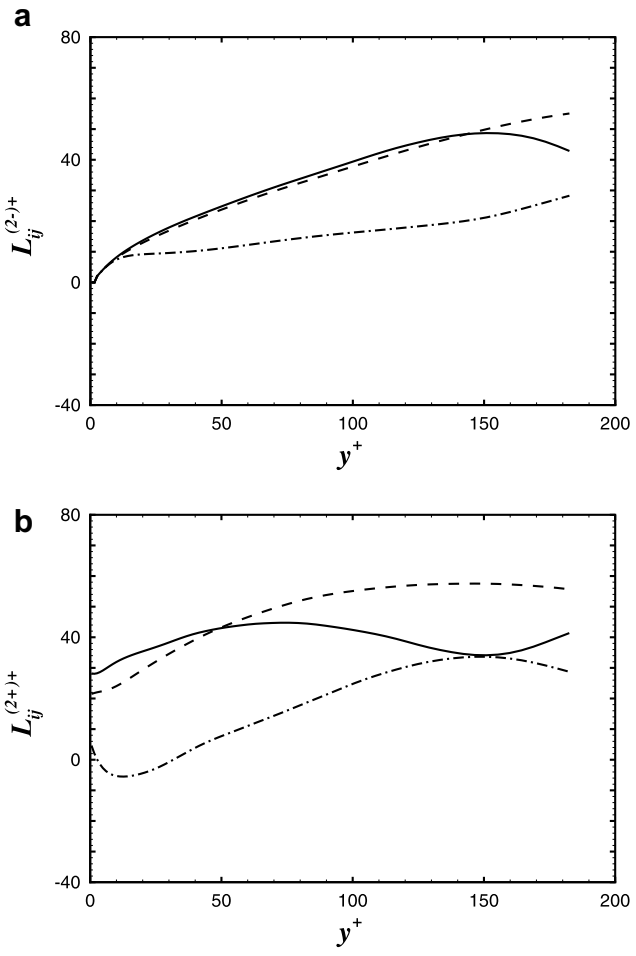

Fig. 2. Wall-normal integral length scales $L_{ij}^{(2)}$. (a) $L_{ij}^{(2-)}$. (b) $L_{ij}^{(2+)}$. (—) $i = j = 1$; (– –) $i = j = 2$; (–·–) $i = j = 3$.

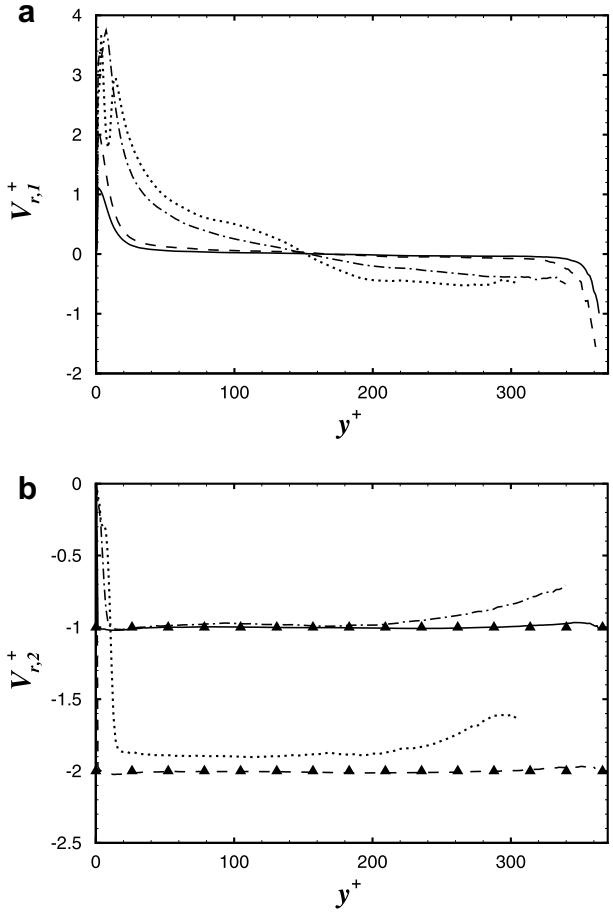

Fig. 3. Mean relative velocity in a horizontal channel flow (bottom wall is located at $y^+ = 0$): (a) streamwise $V_{r,1}$; (b) wall-normal $V_{r,2}$. $\tau_p^+ g^+ = 1$: (—) $\tau_p^+ = 1.2$; (– –) $\tau_p^+ = 15.4$. $\tau_p^+ g^+ = 2$: (– –) $\tau_p^+ = 1.2$; (···) $\tau_p^+ = 15.4$. Terminal velocity: (▲) $\tau_p^+ g^+ = 1$ and 2.

values of all these length scales vary between 0 and 50 in wall units, except $L_{11}^{(1)}$ which can be of the order of the channel half-width.

5. Prediction of the decorrelation time scales of the fluid seen

5.1. Test in a horizontal channel flow

In this configuration, the gravity vector is parallel to Ox_2 and directed from the upper to the lower walls. Before to present the comparison between results issuing from the proposals, i.e. Eqs. (2) and (3), and the DNS results, we propose to show the influence of the gravity on the mean relative velocity. In Fig. 3, the mean relative velocity, $V_{r,i} = \langle v_i - \tilde{u}_i \rangle$, is reported for several values of the particle inertia τ_p^+ and of the dimensionless gravitational acceleration parameter $\tau_p^+ g^+$. Only statistics for which a significant amount of data was collected are presented in this figure. This explains the lack of results near the upper wall located at $y^+ \approx 370$. From Fig. 3(b), it can be observed that the mean relative velocity in the gravity direction (along Ox_2) is equal to the terminal velocity $\tau_p^+ g^+$ when the particle inertia is low whereas for higher particle inertia, the mean relative velocity is smaller. This difference is more pronounced for the higher gravitational acceleration intensity case in which the mean relative velocity can be found to be 10% smaller than the terminal velocity. In Fig. 3(a) related to the streamwise mean relative velocity, we can observed that this component can be important for the highest particle inertia. In the near-wall region, there is an increase of the streamwise mean relative velocity which is more important for the highest particle inertia. In the rest of the channel, a zero value of this mean relative velocity is noted for the lightest particles contrary to the heaviest particles case.

Therefore, the mean relative motion is inclined towards the streamwise axis Ox_1 and thus not strictly aligned with the gravity direction. We have chosen to express Eqs. (2)

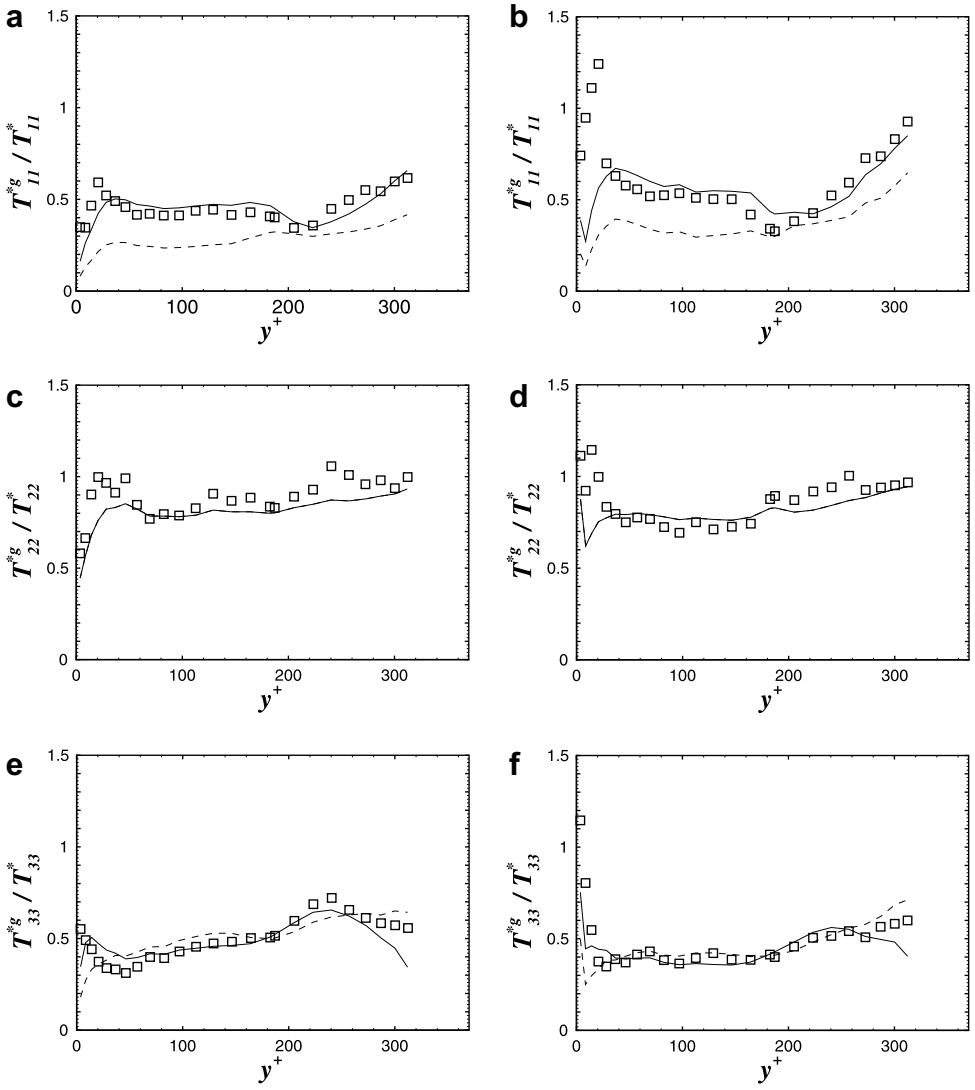

Fig. 4. Decorrelation time scales of the fluid seen in a horizontal channel for $\tau_p^+ g^+ = 1$. (a, c and e): $\tau_p^+ = 1.2$. (b, d and f) $\tau_p^+ = 15.4$. (□) present DNS results; (—) Eq. (2); (––) Eq. (3).

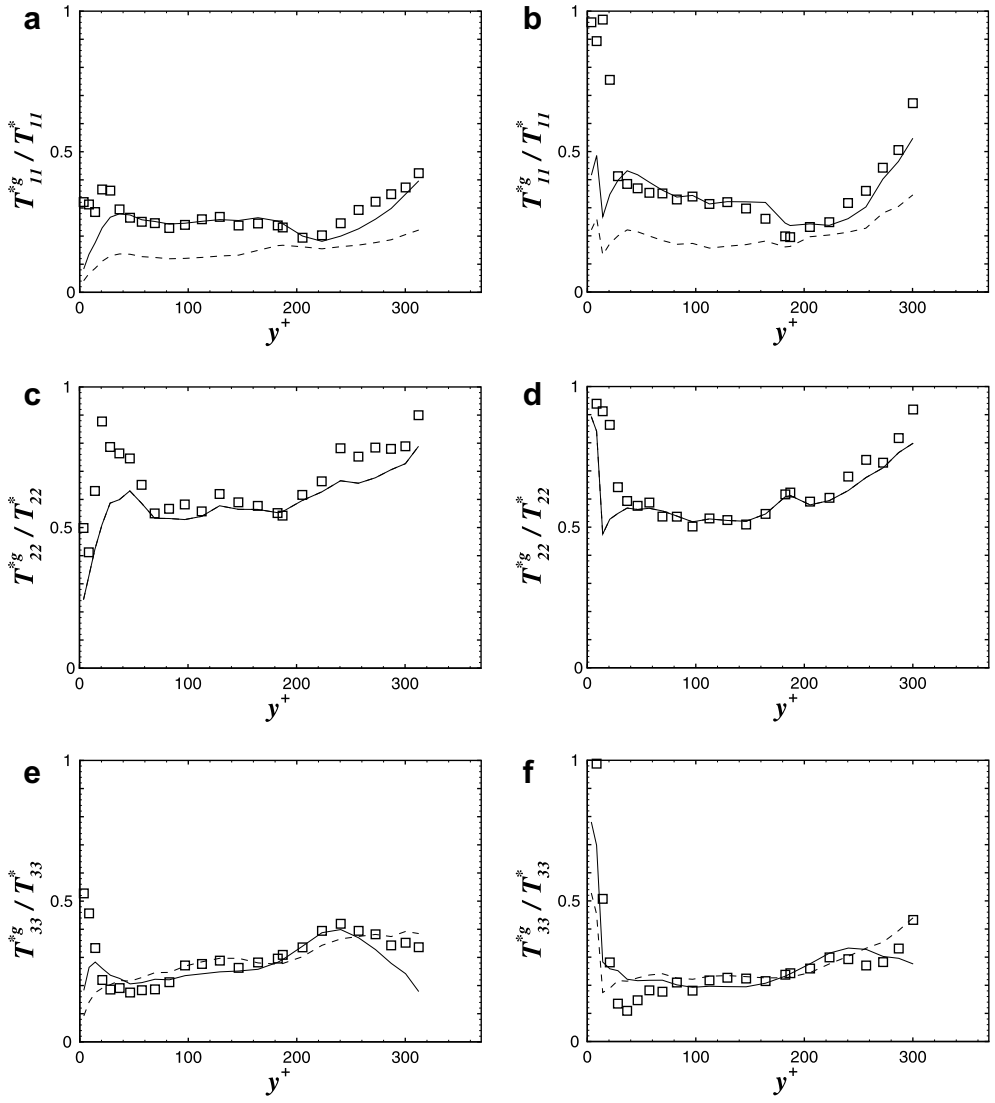

Fig. 5. Decorrelation time scales of the fluid seen in a horizontal channel for $\tau_p^+ g^+ = 2$. (a, c and e): $\tau_p^+ = 1.2$. (b, d and f): $\tau_p^+ = 15.4$. (□) present DNS results; (—) Eq. (2); (––) Eq. (3).

and (3) in a reference system aligned with gravity. Therefore, we implicitly consider that the influence of the crossing trajectory effect on the decorrelation time scales of the fluid seen is mainly due to the wall-normal mean relative velocity. This choice was made since the absolute values of $V_{r,2}$ are greater than those of $V_{r,1}$ almost everywhere in the channel whatever the particle inertia and the values of $\tau_p^+ g^+$. Besides, the performance of Eqs. (2) and (3) to predict the crossing trajectory and continuity effects will be investigated for $V_{r,2}/\langle u_2'^2 \rangle^{1/2} \in [1,3]$.

In Fig. 4 and also in Fig. 5, the ratios T^{*g}_{ii}/T^{*}_{ii} are plotted as a function of y^+ for $\tau_p^+ g^+ = 1$ and $\tau_p^+ g^+ = 2$, respectively. It has to be noted that the results for T^{*}_{ii} used in this study can be found in Arcen et al. (2004). The first observation that can be made is about the decrease of the decorrelation time scales which is of the same order in the streamwise and transverse directions and less important in the wall-normal direction. This is in accordance with the findings of Csanady (1963) who showed that the decrease of the time scales of the fluid seen should be less important in the direction parallel to the mean relative velocity due to the continuity effect. Moreover, from the comparison with the results obtained for $\tau_p^+ g^+ = 2$ (see Fig. 5), it can be noticed that an increase of the gravity acceleration induces a stronger decrease in the decorrelation time scales of the fluid seen. Concerning the inertia effect, it can be seen that whatever the values of $\tau_p^+ g^+$, the influence of the particle inertia is not significant on the ratio T^{*g}_{ii}/T^{*}_{ii}, except may be in the near wall region. However, this does not mean that T^{*g}_{ii} are independent of particle inertia. The results issuing from Eqs. (2) and (3) are also plotted in these figures. It has to be noted that the values of the length scales $L^{(2-)}_{ii}$ are used in these latter expressions since the vertical motion of the particles is mainly directed from the upper wall towards the bottom wall. A good accordance with the DNS results is obtained for T^{*g}_{22}/T^{*}_{22} and T^{*g}_{33}/T^{*}_{33} when Eq. (3) is used. It

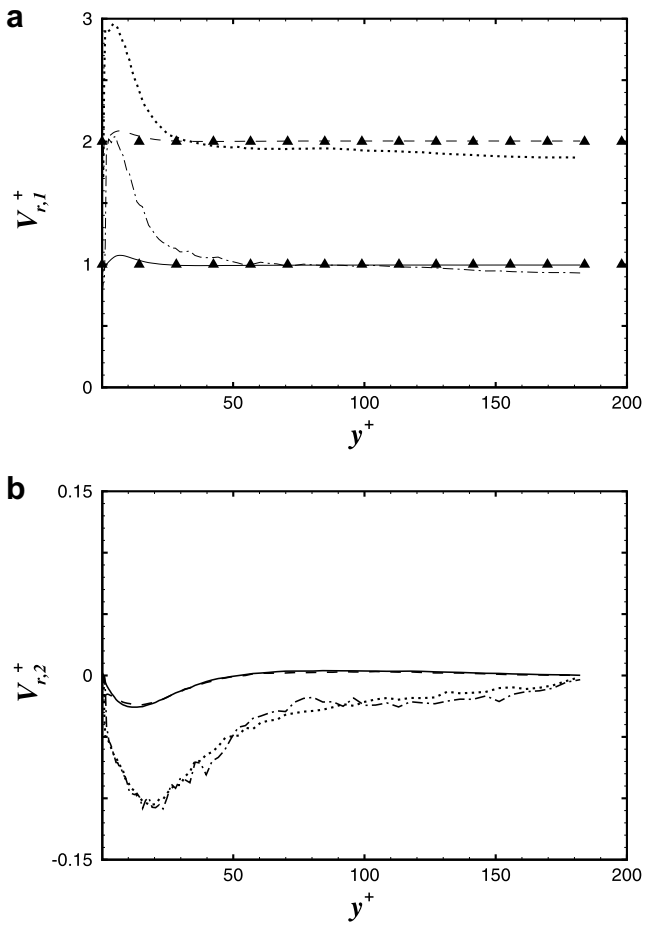

Fig. 6. Mean relative velocity in a downward vertical channel flow: (a) streamwise; (b) wall-normal. $\tau_p^+ g^+ = 1$: (—) $\tau_p^+ = 1.2$; (–·–) $\tau_p^+ = 15.4$. $\tau_p^+ g^+ = 2$: (––) $\tau_p^+ = 1.2$; (···) $\tau_p^+ = 15.4$. Terminal velocity: (▲), $\tau_p^+ g^+ = 1$ and 2.

should be also noticed that the results issuing from Eq. (3) for T_{22}^{*g}/T_{22}^{*} cannot be distinguished since they are identical to those obtained from Eq. (2). Concerning the prediction of T_{11}^{*g}/T_{11}^{*}, some discrepancies appear using Eq. (3) whatever the value of gravity acceleration, i.e. $\tau_p^+ g^+ = 1$ and $\tau_p^+ g^+ = 2$. This can be explained by the fact that the crossing trajectory effects in Eq. (3) is based on relation which is only valid in isotropic turbulent flow. Better results are obtained using Eq. (2) which are directly function of the longitudinal or lateral length scales. Moreover, these expressions give results in a very good accordance with those issuing from DNS for all the components of the time scale of the fluid seen and whatever the intensity of the gravity force. Therefore, the crossing trajectory and the continuity effects can be correctly predicted through the use of Eq. (2) in a large part of the horizontal channel flow.

The disagreement between DNS results and those issuing from Eq. (2) is seen to be significant close to the wall. For $y^+ < 20$, the DNS computation shows that the ratio T_{ii}^{*g}/T_{ii}^{*} increases and can be higher than unity whereas the values predicted by Eq. (2) are lower than unity (see Fig. 4). This trend is more pronounced for the heaviest particle inertia $\tau_p^+ = 15.4$ and for the lowest value of the dimensionless gravity acceleration, i.e. $\tau_p^+ g^+ = 1$. It can be observed that for this inertia T_{11}^{*g}/T_{11}^{*} increases up to 1.3, whereas the maximum value of T_{33}^{*g}/T_{33}^{*} and T_{22}^{*g}/T_{22}^{*} is about 1.1. In other words, in this part of the channel, the decrease of the correlation of the fluid fluctuating velocity along the particle trajectory is less rapid in the presence of gravity than in its absence. A possible explanation is that the range of the statistical properties of the turbulence experienced by the particles is less important when the gravity force is acting. Indeed, gravity prevents most of the particles to move outside the near-wall region and thus induces an increase of the particle residence time in this zone. Moreover, it should be noted that the lift is also responsible for the increase of the particle residence time near the bottom wall since the gravity induces a large mean streamwise relative velocity in a region of strong wall-normal gradient of the streamwise fluid velocity.

5.2. Test in a downward vertical channel flow

Before to present the results obtained using Eqs. (2) and (3) in a downward vertical channel flow, the direction of the mean relative motion has to be studied in order to choose the appropriate length scales which will be used in these expressions. The mean streamwise relative velocity as well as the terminal velocity of a solid particle in a quiescent gas flow are plotted in Fig. 6(a) for two values of the particle inertia and of the intensity of the gravity acceleration. The mean relative velocity for the lightest particles is identical to the terminal velocity whatever the intensity of the gravity force whereas this is not the case for the highest particle inertia. For these particles, there is a rapid increase of the mean streamwise relative velocity at $y^+ \lesssim 5$. This behavior has been already seen by Rouson and Eaton (2001) in the same flow configuration. In the wall-normal direction, see Fig. 6(b), the mean relative velocity is seen to be small but not equal to zero for the heaviest particles whatever the intensity of the gravity force, whereas the values obtained in the case of the lightest particle evolve around zero, except in the near-wall region. Consequently, the mean relative velocity vector is slightly inclined towards the wall. Nevertheless, the value of $V_{r,1}$ is found to be, at the minimum, 10 times higher than the absolute value of $V_{r,2}$. This has leads us to consider that the mean relative motion is mainly parallel to the streamwise direction. Therefore, we have applied Eqs. (2) and (3) using the mean relative streamwise velocity $V_{r,1}$ in association with the length scales $L_{ii}^{(1)}$. The performance of Eqs. (2) and (3) to predict the crossing trajectory and continuity effects will be investigated for $V_{r,1}/\langle u_1'^2 \rangle^{1/2} \in [0.5, 2.5]$. The results obtained for the decorrelation time scales of the fluid seen in a downward vertical channel flow are presented in Fig. 7 and also in Fig. 8 for $\tau_p^+ g^+ = 1$ and $\tau_p^+ g^+ = 2$, respectively. As observed in the horizontal channel flow configuration, a decrease of the decorrelation time scales of the fluid seen is noted and it appears more important in the direction

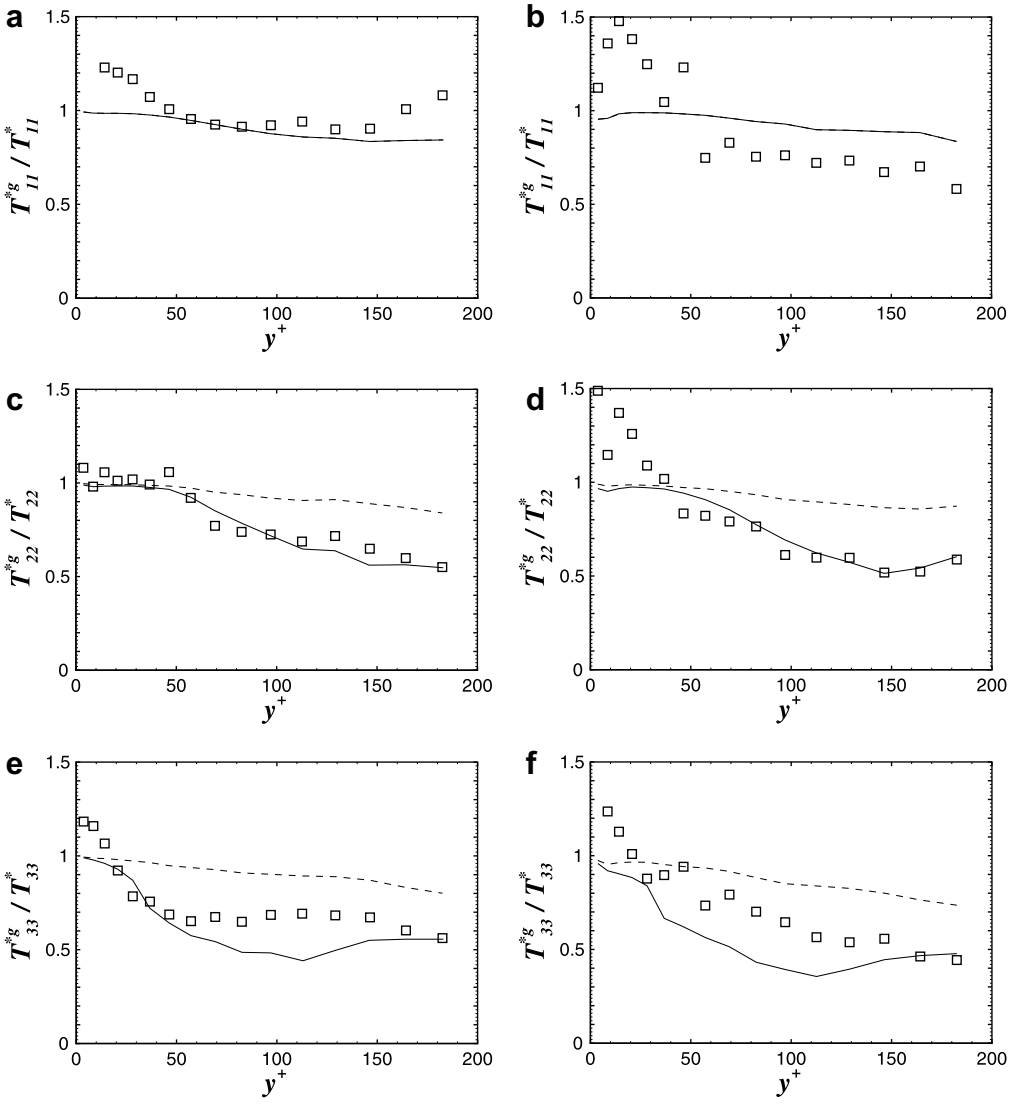

Fig. 7. Decorrelation time scales of the fluid seen in a downward vertical channel flow for $\tau_p^+ g^+ = 1$. (a, c and e): $\tau_p^+ = 1.2$. (b, d and f): $\tau_p^+ = 15.4$. (□) present DNS results; (—) Eq. (2); (––) Eq. (3).

parallel to the gravity whatever the particle inertia and the intensity of the gravity force. Nevertheless, the difference in the decrease of the time scales of the fluid seen in the direction parallel and perpendicular to the gravity is less pronounced than in the horizontal channel flow. This is probably due to the fact that, in contrary to the horizontal channel flow configuration, the ratio $T^*_{ii}/L^{(i)}_{ii}$ is not significantly different to the one obtained in the perpendicular directions to the mean relative velocity, i.e. $T^*_{jj}/L^{(i)}_{jj}$. However, we note that for the highest values of the mean relative velocity, the decrease of the decorrelation time scales of the fluid seen is more important. In comparison to the horizontal case, the values of these time scales have similar trends with respect to the intensity of the gravity force.

Furthermore, as observed in the horizontal channel flow case, T^{*g}_{ii} can be found to be higher than T^*_{ii} in the near wall region. Nevertheless, this trend is observed whatever the particle inertia and the intensity of gravity acceleration in this flow configuration. As explained before, this effect can be attributed to the fact that particles spend more time in the wall region in the presence of the gravity. The increase of the particle residence time in this part of the channel is certainly due to the lift force which is directed towards the wall. The effect of the lift force is more important in the presence of gravity since it induces a mean streamwise relative velocity which is larger than in its absence.

Concerning the capability of the different models, Eqs. (2) and (3), to predict the crossing trajectory and continuity effects, we observe from Fig. 7 and also in Fig. 8, that the decrease of T^{*g}_{11}/T^*_{11} is well predicted by these two couples of expressions whatever the particle inertia and the values of $\tau_p^+ g^+$ in a large part of the channel flow. Nevertheless, a better estimate is obtained for T^{*g}_{22}/T^*_{22} when Eq. (2) is used, since the decrease predicted by Eq. (3) is not enough important. It is interesting to note that in opposite to the

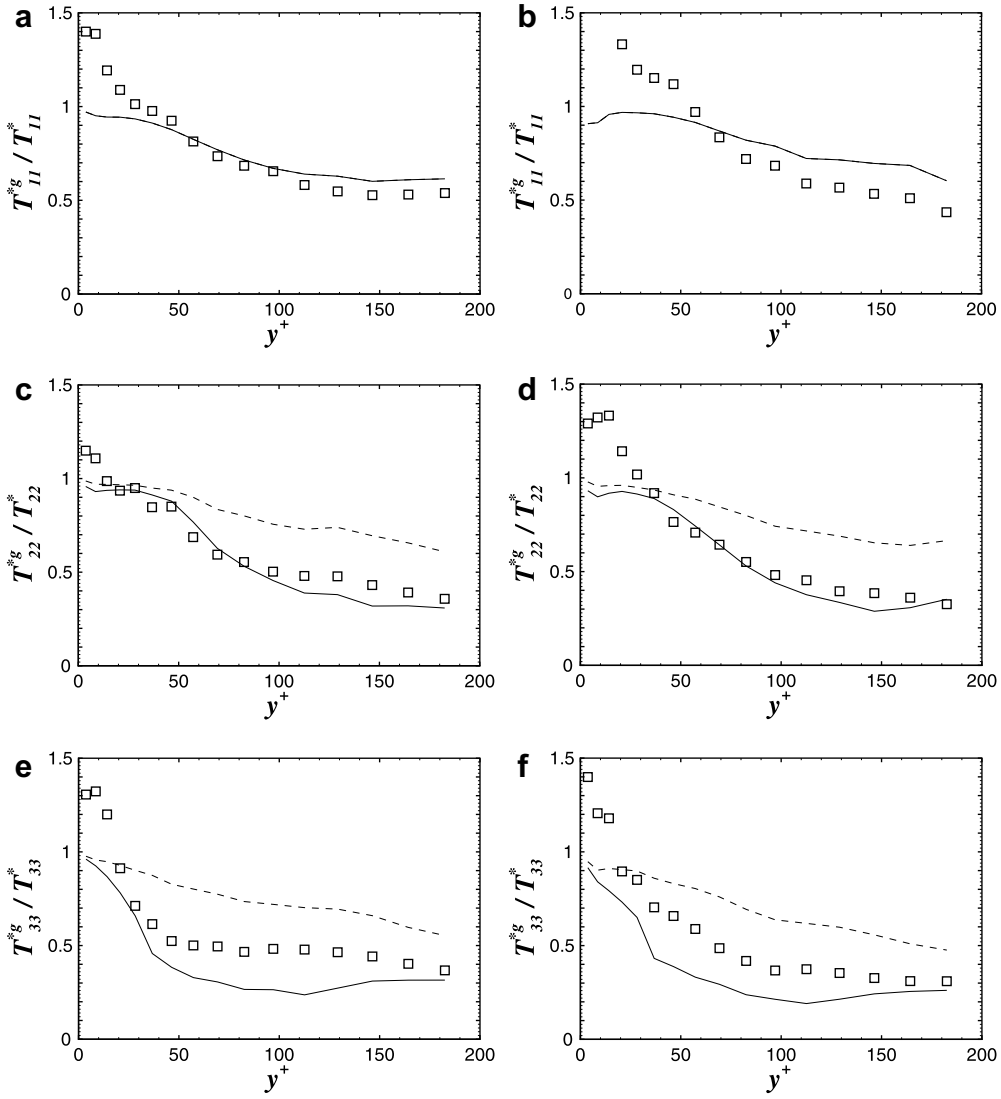

Fig. 8. Decorrelation time scales of the fluid seen in a downward vertical channel flow for $\tau_p^+ g^+ = 2$. (a, c and e): $\tau_p^+ = 1.2$. (b, d and f): $\tau_p^+ = 15.4$. (□) present DNS results; (—) Eq. (2); (––) Eq. (3).

horizontal channel flow, Eq. (3) underestimates the influence of the crossing trajectory effect on the decorrelation time scales of the fluid seen. As it can be seen, none of these expressions seems to be able to predict accurately the decrease of the time scale T^{*g}_{33}/T^{*}_{33} in opposite to the results obtained in a horizontal configuration. However, on the whole, Eq. (2) yields better prediction.

6. Discussion and conclusion

DNS simulation of a cloud of solid particles in horizontal and downward vertical channel flows clearly shows a decrease of the decorrelation time scales of the fluid seen which is more important in the directions perpendicular to the mean relative velocity. The crossing trajectory and continuity effects predicted for isotropic turbulence by Yudine (1959) and Csanady (1963) are qualitatively identical to those observed in non-homogeneous turbulence. The use of similar expressions to those proposed by Csanady (1963) in order to model the influence of these two effects on the decorrelation time scales of the fluid seen appears to be possible.

Two couples of expressions derived from Csanady (1963) that include the anisotropic character of the turbulence, the inertia and continuity effects have been proposed. The couple of expressions, Eq. (3), is quite close to the one proposed by Csanady since the continuity effect is taken in a similar way, i.e. the longitudinal length scale is considered to be twice higher than the lateral length scales. The expressions of the proposal, Eq. (2), are directly function of the longitudinal or lateral length scales. The comparison between the DNS results and those provided by these expressions has revealed that Eq. (2) is able to successfully model the decrease of the time scales of the fluid seen except in the near-wall region. The prediction issuing from Eq. (3) are less satisfactory since these expressions overes-

timate the crossing trajectory effect in the horizontal channel flow and underestimate it in the downward vertical channel flow configuration. In the near-wall region, none of the proposed expressions give satisfactory results since DNS results reveal an increase of the decorrelation time scales of the fluid seen which can become higher than the decorrelation time scales obtained in the absence of gravity.

This study also shows that the use of a simple functional form including good estimate of the parameters that enter this functional expression is satisfactory. Nonetheless, the major drawback of this new proposal is that it necessitates to know beforehand the spatial two-points characteristics of the turbulence and the decorrelation time scales of the fluid seen when no external force is acting on particles. Unfortunately, no models of these two latter characteristics exist for non-homogeneous turbulence. Further studies of these parameters are thus needed to improve the models of the crossing trajectory and continuity effects in shear flows.

Moreover, in contrary to the study of Csanady in an homogeneous turbulence, the present DNS results show that the mean relative velocity vector is not collinear with the gravity acceleration vector. It has to be kept in mind that in order to apply Csanady's theory, the reference system has to be chosen so that the mean relative motion is aligned with one of its axes. This last condition could not has been fulfilled in our case. Therefore, it has lead us to assume that the mean relative motion in the horizontal and downward channel flows is parallel to the gravity direction and thus aligned with one of the axes of the reference system. However, the directions, namely $\mathbf{g}/\|\mathbf{g}\|$ and $\mathbf{V}_r/\|\mathbf{V}_r\|$, have to be distinguished in real flows like in an non-homogeneous flow. In the absence of any external force, a separation of the average trajectories of the discrete and of the fluid elements is observed due to particle inertia effect and therefore, a mean relative velocity exists (see the study by Arcen et al. (2004) in a channel flow). In the presence of an external force field, the mean relative velocity, induced by inertia effect, still exists. Nevertheless, its magnitude can become more important due to the external force (i.e. gravity). We think that the direction of the mean relative velocity, with or without an external force, is the most important one. Consequently, the correct approach would be thus to express our proposal in a reference system aligned with $\mathbf{V}_r/\|\mathbf{V}_r\|$ and then to use rotation matrices to change to an arbitrary reference system. An improvement of the present work would be to extend the formalism of the new proposal to a tensorial form in order to predict the crossing trajectory effect independently of the relative motion direction. A generalization for the case where $\mathbf{V}_r$ has any orientation with respect to the coordinate system has been already proposed by Simonin et al. (1993) and Minier and Peirano (2001) for isotropic turbulence. The main difficulty arising from this approach is to define a tensorial form of the length scales in a non-homogeneous flow. The extension of the formalism to non-homogeneous turbulent flows should be the next step of the present work.

Acknowledgements

The authors thank Jean-Pierre Minier and Benoît Oesterlé for many stimulating and helpful discussions on the crossing trajectory effect.

References

Arcen, B., Tanière, A., Oesterlé, B., 2004. Numerical investigation of the directional dependance of integral time scales in gas–solid channel flow. In: Proceedings of the Fifth International Conference on Multiphase Flow, Paper No. 297, Yokohama, Japan.

Arcen, B., Tanière, A., Oesterlé, B., 2006. On the influence of near-wall forces in particle-laden channel flows. Int. J. Multiphas. Flow 32, 1326–1339.

Comte-Bellot, G., 1965. Écoulement turbulent entre deux plaques planes parallFles. Publications scientifiques et techniques du ministére de l'air Paris, PST 419.

Csanady, G.T., 1963. Turbulent diffusion of heavy particles in the atmosphere. J. Atmos. Sci. 20, 201–208.

Derevich, I.V., 2000. Statistical modelling of mass transfer in turbulent two-phase dispersed flows. Int. J. Heat Mass Transfer 43, 3709–3723.

Derevich, I.V., 2001. Influence of internal turbulent structure on intensity of velocity and temperature fluctuations of particles. Int. J. Heat Mass Transfer 44, 4505–4521.

Deutsch, E., 1992. Dispersion de particules dans une turbulence homogéne isotrope stationnaire calculée par simulation numérique des grandes échelles. Ph.D. thesis, Ecole centrale de Lyon, Collection des notes internes de la DER, Electricité de France, Clamart, France.

Grant, H., 1958. The large eddies of turbulent motion. J. Fluid Mech. 4, 149–190.

Iwamoto, K., 2002. Database of Fully Developed Channel Flow. Rapport No. ILR-0201, THTLAB. Department of Mechanical Engineering, The University of Tokyo.

Kim, J., Moin, P., Moser, R., 1987. Turbulence statistics in fully developed channel flow at low Reynolds number. J. Fluid Mech. 177, 133–166.

Kristoffersen, R., Andersson, H.I., 1993. Direct simulations of low-Reynolds-number turbulent flow in a rotating channel. J. Fluid Mech. 256, 163–197.

Marchioli, C., Soldati, A., Kuerten, J.G.M., Arcen, B., Taniére, A., Goldensoph, G., Squires, K.D., Cargnelutti, M.C., Portela, L.M., in press. Statistics of particle dispersion in direct numerical simulations of wall-bounded turbulence: results of an international collaborative benchmark test. Int. J. Multiphas. Flow., in press.

Minier, J.P., Peirano, E., 2001. The PDF approach to turbulent polydispersed two-phase flows. Phys. Rep. 352, 1–214.

Minier, J.P., Peirano, E., Chibbaro, S., 2004. PDF model based on Langevin equation for polydispersed two-phase flows applied to a bluff-body gas–solid flow. Phys. Fluids 16, 2419–2431.

Moser, R., Kim, J., Mansour, N., 1999. Direct numerical simulation of turbulent flow in a channel up to $Re_\tau = 590$. Phys. Fluids 11, 943–945.

Oesterlé, B., Zaichik, L.I., 2004. On Lagrangian time scales and particle dispersion modeling in equilibrium shear flows. Phys. Fluids 16, 3374–3384.

Orlandi, P., 2000. Fluid Flow Phenomena. A Numerical Toolkit. Kluwer Academic Publishers.

Reeks, M.W., 2005. On probability density function equations for particle dispersion in a uniform shear flow. J. Fluid Mech. 522, 263–302.

Reynolds, A.M., 2004. Stokes number effects in Lagrangian stochastic models of dispersed two-phase flows. J. Colloid Interface Sci. 275, 328–335.

Rouson, D.W.I., Eaton, J.K., 2001. On the preferential concentration of solid particles in turbulent channel flow. J. Fluid Mech. 428, 149–169.

Sawford, B.L., Guest, F.M., 1991. Lagrangian statistical simulation of the turbulent motion of heavy particles. Boundary-Layer Meteorol. 54, 147–166.

Simonin, O., 2000. Statistical and Continuum Modelling of Turbulent Reactive Particulate Flows. Lecture Series 2000–2006. von Karman Institute for Fluid Dynamics, Belgium.

Simonin, O., Deutsch, E., Minier, J.P., 1993. Eulerian prediction of fluid–particle correlated motion in turbulent two-phase flows. Appl. Sci. Res. 51, 275–283.

Thomas, L., Oesterlé, B., 2005. An investigation of crossing trajectory effects in turbulent shear flow. In: Proceeding of ASME Fluids Engineering Division Summer Meeting and Exhibition, FEDSM05, vol. 1, Houston, USA, pp. 703–712.

Wang, L., Stock, D.E., 1993. Dispersion of heavy particles by turbulent motion. J. Atmos. Sci. 50, 1897–1913.

Wilson, J.D., 2000. Trajectory models for heavy particles in atmospheric turbulence: comparison with observations. J. Appl. Meteorol. 39, 1894–1912.

Yudine, M.I., 1959. Physical considerations on heavy-particle dispersion. Adv. Geophys. 6, 185–191.